

Effect of Crystallographic Orientation on the Corrosion Behavior of Mo₃Si Single Crystals in NaCl Solution

R. Lopez-Sesenes¹, I. Rosales², J. Uruchurtu-Chavarin², V.M. Salinas-Bravo³,
J.G. González-Rodríguez^{2*}

¹ Universidad Autónoma del Estado de Morelos, FCQeI., Av. Universidad No. 1001, Col. Chamilpa, Cuernavaca, Morelos, Mexico. C.P. 62209.

² Universidad Autónoma del Estado de Morelos, CIICAp. Av. Universidad No. 1001, Col. Chamilpa, Cuernavaca, Morelos, Mexico. C.P. 62209.

³ Instituto Nacional de Electricidad y Energías Limpias, Interior Internado Palmira, Cuernavaca, Mor., Mexico

*E-mail: ggonzalez@uaem.mx

Received: 22 January 2018 / Accepted: 20 February 2018 / Published: 10 April 2018

The corrosion behavior of polycrystalline and Mo₃Si single crystal in its crystal orientations, namely [100], [110] and [111] was evaluated in 0.05 and 0.5 M NaCl solutions. For this, electrochemical impedance spectroscopy, (EIS), potentiodynamic polarization curves, and electrochemical noise analysis (ENA) were used. Parameters calculated from the different techniques such as polarization, noise, and charge transfer resistance had a highest value for the [100] single crystal, whereas the lowest value was for the polycrystalline material. Although single crystals exhibited a higher corrosion resistance than polycrystal, all the different materials were highly susceptible to pitting corrosion. This difference in corrosion behavior was explained in terms of difference in surface energy values and in the number of atom density.

Keywords: Molybdenum silicides, single crystals, corrosion, crystal orientation, corrosion, electrochemical techniques.

1. INTRODUCTION

Silicide alloys have been widely studied due to its physical and mechanical properties which provide important characteristics when they are combined with other materials. In this direction, molybdenum silicides have been employed as corrosion protective coating materials at high temperatures and it is considered the most promissory candidates for this application, together with other properties such as strength, creep resistance, oxidation resistance and mechanical and

microstructural stability which make these compounds a material with high potential in application at high temperature in turbine airfoils, burning chambers parts among others [1-3].

Mo₃Si has received a great deal of attention focusing on the growth mode and possible intermixing in the interface region, silicide formation, and the characterization of the electronic densities in the few first interface layers. Johanson [4] reported a study where the growth mode was induced in the Mo₃Si at (100) and (110) with the purpose to observe the electronic and structural properties of these materials where a change in the level energy was observed based on the surface orientation.

Different authors have reported the influence of the crystal-orientation on the corrosion behavior of several materials such as Alloy 690, Mg, Mg-Al, Fe₂B and AISI 340 austenitic stainless steel. Wang found that the corrosion rate is dependent on the surface free energy and crystal orientation [5-7]. Shin [8] studied the effect of the crystallographic orientation on the corrosion resistance of magnesium single crystal determining that an increase in the rotation angle close to 0 or 90 degrees in the planes affect the corrosion rate. Fan [9] studied the effect of crystal orientation on the aluminum anodes of aluminum-air batteries observing that the resistance and corrosion rate is clearly depending on the crystallographic orientation. Latief [10] studied the effect of crystal orientation on the oxidation resistance of CM186LC Ni-based superalloy at 1100°C in air, finding a different oxidation rate for the different crystal orientations. In the case of Mo₃Si do not exist reports concerning the crystal orientation effect on its corrosion rate, however, several researchers have focused in improving its physical and mechanical properties as well as the effect of other chemical elements and thermal treatments when immersed in acid and neutral solutions used as electrolytes [2, 11-16]. Therefore the objective of the present work is to determine the effect the different of the Mo₃Si crystal orientations on its corrosion behavior immersed in NaCl at two different concentrations such as 0.5 and 0.05 M.

2. EXPERIMENTAL PROCEDURE

2.1 Materials.

Mo₃Si alloys with single-phase composition were arc-melted under an argon atmosphere using high-purity elements (Mo 99.999% and Si 99.99% purity). Alloys were arc-melted by using a copper-finger mold with dimensions of 90 mm length and 15 mm depth. Crystal growth procedure (optical floating zone method) is mentioned in a previous work [17], and by Laue back reflection technique the growth direction of as-grown crystal was identified to be close to <102>, and using a goniometer, three new crystals with different orientations, namely <111>, <110> and <100> were cut by EDM (electro discharge machine) technique. For corrosion tests, polycrystalline Mo₃Si was used as reference sample with an exposed area of 6.625 10⁻² cm². Then, the three new crystallographic orientations of Mo₃Si, (100), (110), and (111) were used with an exposed area of 5.68 10⁻², 6.44 10⁻² and 5.11 10⁻² cm² respectively. Samples were embedded in epoxy resin and abraded with 1000 grade emery paper,

washed with distilled water, degreased with acetone and dried with cool flowing air to ensure a reproducible initial condition for each experiment.

2.2 Methods.

Electrochemical experiments were carried out to evaluate the corrosion behavior of the Mo_3Si polycrystal and its different crystallographic orientation at room temperature in 0.5 and 0.05 M NaCl solutions prepared with distilled water. The electrochemical measurements consisted of Potentiodynamic polarization curves, Electrochemical noise (EN), and Electrochemical impedance spectroscopy (EIS) measurements, which were employed to evaluate the corrosion behavior of samples under evaluation. All electrochemical tests were carried out in a conventional three electrodes cell where a graphite rod was used as a counter electrode, and a Ag/AgCl electrode as reference electrode. All measurements were carried out at least three times. Potentiodynamic polarization curves were done by polarizing the specimen starting from -1000 up to 1000 mV with respect to free corrosion potential, E_{corr} , at a scanning rate of 1 mV/s in an ACM Instruments potentiostat. The corrosion current density values, I_{corr} were obtained by using Tafel extrapolation. EIS measurements were performed in a PC4 300 Gamry potentiostat at the open circuit potential with the application of a signal with an amplitude of 10 mV in a range of frequency of 10^{-2} to 10^3 Hz with 10 points per decade. EN readings in both current and in potential were done by using two nominally identic working electrodes [17]. Reading blocks with a total of 1024 points were recorded in current and potential through time by using a zero-resistance ammeter (ZRA) from ACM instruments. Trend removal of the data was performed for this by using a least square fitting method.

3. RESULT AND DISCUSSION

3.1 Potentiodynamic Polarization Curves.

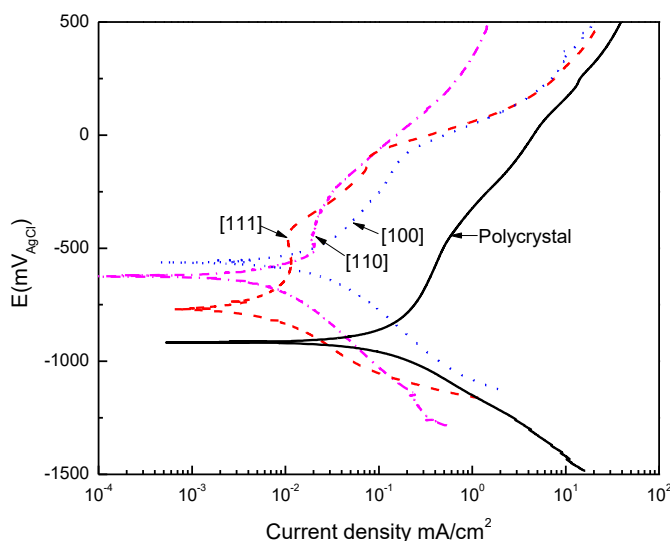


Figure 1. Potentiodynamic polarization curves for Mo_3Si polycrystal and single crystals immersed in 0.05 M NaCl.

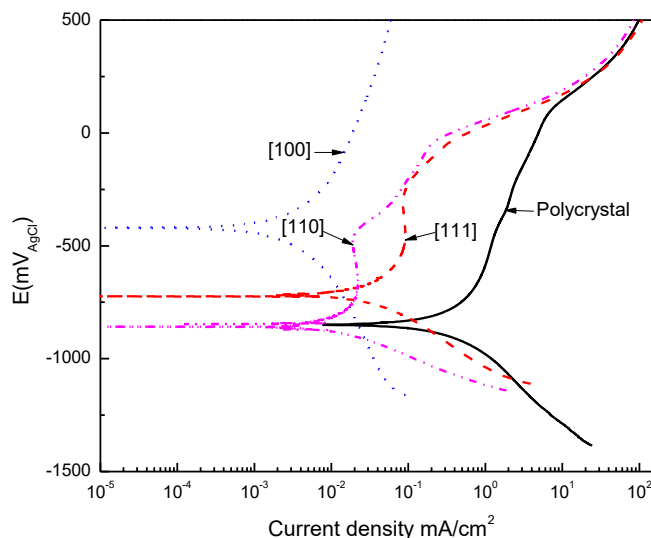


Figure 2. Potentiodynamic Polarization curves for Mo₃Si polycrystal and single crystals immersed in 0.5 M NaCl.

Polarization potentiodynamic curves were performed in 0.05 and 0.5 M NaCl solutions. Polarization curves in 0.05 M NaCl solution, Fig. 1, shows an active-passive behavior for all the materials. The passive behavior could be due to the formation of oxides such as SiO₂, Mo₅Si₃ and Mo₃Si [18-20]. Due to the fact that the oxidation resistance results from the formation of a highly protective SiO₂ layer in MoSi₂-containing alloys, molybdenum silicides have been intensively studied and it has been reported that the obtained oxide film under thermal oxidation conditions is similar to that obtained upon anodic oxidation[18]. Similarly, in another research work [19] it was concluded that no protective SiO₂ film was formed on molybdenum silicides. In another work, MoSi₂ was corroded in acidic media and it was found that the passivation could be due to the formation of hydrated oxides[18], and when plasma-sprayed MoSi₂ in sulfuric acid solution was evaluated, it was reported that the passive film was made mainly of SiO₂[20].

Table 1. Parameters obtained from potentiodynamic polarization curves for Mo₃Si polycrystal and single crystals immersed in 0.05 M NaCl.

Sample	E _{corr} (mV _{Ag/AgCl})	I _{corr} (mA/cm ²)	E _{pit} (mV _{Ag/AgCl})	I _{pass} (mA/cm ²)
Polycrystal	-910	1.1 x 10 ⁻¹	-430	3.4 x 10 ⁻¹
[100]	-621	8.86 x 10 ⁻³	-80	6.2 x 10 ⁻²
[110]	-874	6.66 x 10 ⁻³	-230	2.10 x 10 ⁻²
[111]	-578	1.74 x 10 ⁻²	-435	1.1 x 10 ⁻¹

The E_{corr} value of the polycrystal shifted towards nobler values and the I_{corr} value decreased up to two orders of magnitude for the single crystals. Thus, whereas the polycrystal exhibited an E_{corr} value of -910 mV, a value of -578 mV was obtained for [111] single crystal. On the other side, the corrosion current density value for the polycrystalline material was 1.1 x 10⁻¹ mA/cm², that value for

[110] monocrystal was $6.66 \times 10^{-3} \text{ mA/cm}^2$. On the other side, the passive film properties for monocrystals were improved as compared to those obtained with polycrystalline material. Thus, the pitting potential value, E_{pit} , for polycrystal was -430 mV, monocrystals showed higher E_{pit} values, except [111] monocrystal. In addition to this, the passive current density value, I_{pass} , observed in the polycrystal, 3.4 mA/cm^2 , was higher than those values observed in the monocrystals. Table 1 shows a summary of these parameters.

Table 2. Parameters obtained from potentiodynamic polarization curves for Mo_3Si polycrystal and single crystals immersed in 0.5 M NaCl.

Sample	E_{corr} (mV _{Ag/AgCl})	I_{corr} (mA/cm ²)	E_{pit} (mV _{Ag/AgCl})	I_{pass} (mA/cm ²)
Polycrystal	-855	4.65×10^{-1}	93	2.1
[100]	-420	3.1×10^{-3}	---	---
[110]	-852	8.71×10^{-3}	-456	2.1×10^{-2}
[111]	-724	4.73×10^{-2}	-226	8.61×10^{-2}

When the solution concentration was increased up to 0.5 M, Fig. 2 and table 2, the behavior was very similar to that found in 0.05 M NaCl solution: the E_{corr} value was nobler for single crystals than that obtained with polycrystal, and both the I_{corr} and I_{pass} values were lower for single crystals. However, there were two differences: the current density were slightly higher in the more concentrated solution, there was no passive zone observed for [100] monocrystal, and the E_{pit} value was nobler for polycrystalline material than that value obtained for single crystals, whereas in 0.05M NaCl solution the opposite behavior was observed. This difference in the orientation dependence must be related to a difference in activation energy for these cathodic reactions and site density i.e. number of atomic ledges per unit area[21]. Calculated surface energy values were 0.41, 0.38 and 0.28 J/m² for [111], [100] and [110] monocrystals whereas density values of 12.54, 2.12 and 1.73 atoms/nm² for the same monocrystals were obtained.

3.2 EIS measurements.

EIS data for the different Mo_3Si single crystals as well for polycrystalline materials in NaCl solutions are given in Figs. 3 and 4. For the tests in 0.05 M NaCl solutions, Fig. 3 a, Nyquist diagrams show that data describe a depressed, capacitive-like semicircle at high and intermediate frequency values, and a second capacitive semicircle at lower frequencies. The high frequency semicircle corresponds to the double electrochemical layer whereas the lower frequency loop corresponds to the formation of a protective corrosion products layer. On the other hand, Bode diagrams in the impedance mode, Fig. 3 b, indicates that the lowest impedance value corresponds to the polycrystalline material, whereas the highest value is for the [100] single crystal. On the other hand, Bode diagrams in the Phase angle mode, shows the presence of two time constants. The highest angle phase corresponds for the [100] monocrystal, whereas the lowest value was for the polycrystalline material. A very similar

behaviour was observed in 0.5 M NaCl solution, Fig. 4, where once again, it was observed that the impedance values for the polycrystalline material was much lower than that obtained with the monocrystals.

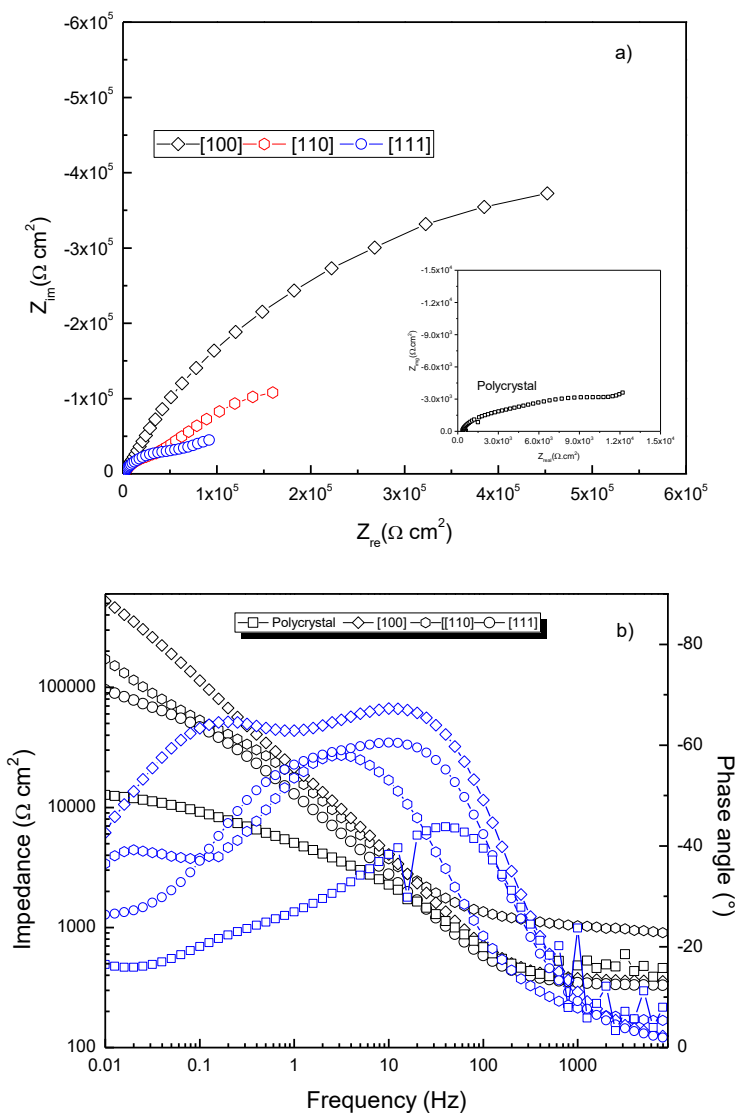


Figure 3. EIS data in the a) Nyquist and b) Bode format for Mo₃Si polycrystal and single crystals immersed in 0.05 M NaCl .

Impedance data were simulated by using electric circuit shown in Fig. 5. In this figure, R_s is the solution resistance, R_f and C_f the corrosion products layer resistance and capacitance, R_{ct} the charge transfer resistance, and C_{dl} the double electrochemical layer capacitance. To take into account the effects of surface heterogeneities such as roughness due to corrosion etc..., a constant phase element, CPE, is placed in terms of an ideal capacitor [22, 23]. The impedance of a CPE is described by the expression:

$$Z_{CPE} = Y^{-1} (iw)^{-n} \tag{1}$$

where Y is the admittance, i is $\sqrt{-1}$, w is $2\pi f$, f the frequency and n is a parameter that gives surface properties such as roughness etc...Parameters obtained from the fitting in 0.05 and 0.5 M NaCl solutions are given in tables 3 and 4 respectively.

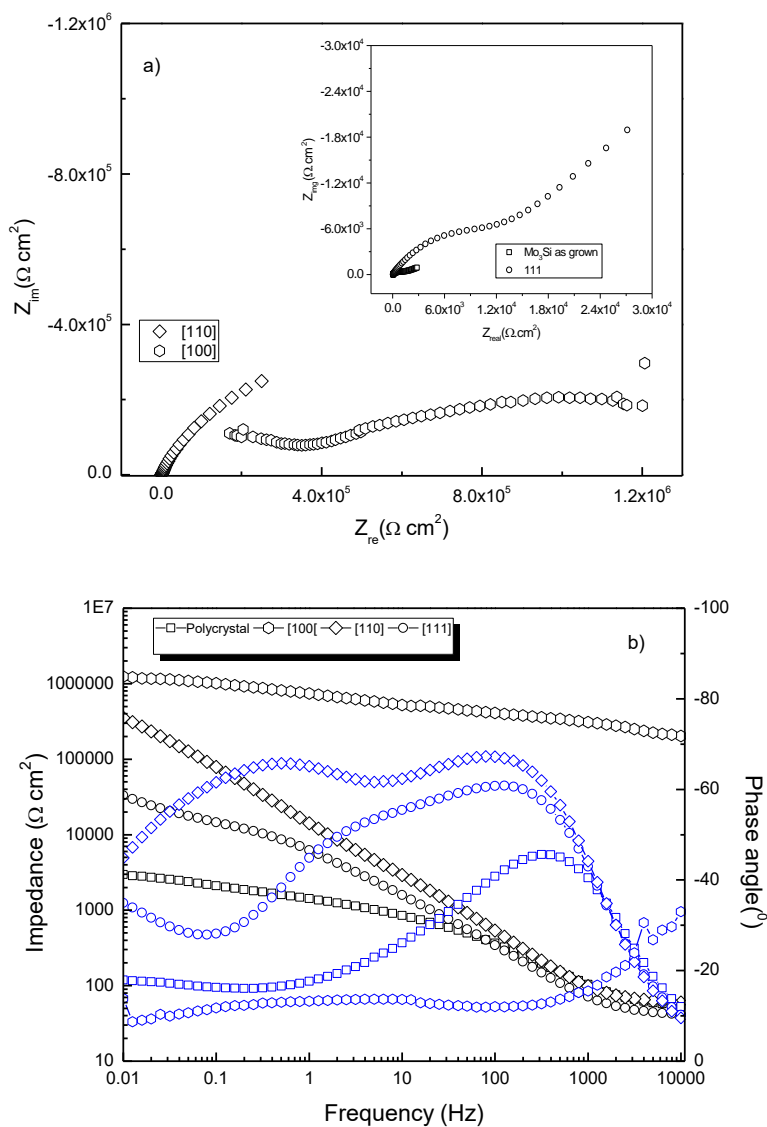


Figure 4. EIS data in the a) Nyquist and b) Bode format for Mo_3Si polycrystal and single crystals immersed in 0.05 M NaCl .

Table 3. Electrochemical parameters used to fit EIS data for Mo_3Si polycrystal and single crystals immersed in 0.05 M NaCl.

Sample	R_s ($\Omega\text{ cm}^2$)	R_{ct} ($\Omega\text{ cm}^2$)	CPE_{dl} (F cm^2)	n_{dl}	R_f ($\Omega\text{ cm}^2$)	CPE_f (F cm^2)	R_p ($\Omega\text{ cm}^2$)	n_f
Polycrystal	4.96×10^2	1.19×10^4	6.01×10^{-6}	0.8	2.18×10^4	5.01×10^{-6}	3.43×10^4	0.5
[100]	3.40×10^2	4.08×10^4	4.64×10^{-6}	0.9	8.76×10^5	6.73×10^{-6}	9.16×10^5	0.8
[110]	9.77×10^2	7.52×10^4	1×10^{-5}	0.8	1.98×10^5	5.64×10^{-5}	2.75×10^5	0.9
[111]	3.16×10^2	5.49×10^4	1.2×10^{-5}	0.8	1.28×10^5	1.79×10^{-4}	1.83×10^5	0.6

Table 4. Electrochemical parameters used to fit EIS data for Mo₃Si polycrystal and single crystals immersed in 0.5 M NaCl.

Sample	R _s (Ω cm ²)	R _{ct} (Ω cm ²)	CPE _{dl} (F cm ²)	n _{dl}	R _f (Ω cm ²)	CPE _f (F cm ²)	R _p (Ωcm ²)	n _f
Polycrystal	5.02 x 10 ¹	3.21 x 10 ²	2.62 x 10 ⁻⁶	0.8	1.09 x 10 ³	1.94 x 10 ⁻⁵	2.88 x 10 ³	0.4
[100]	2.83x 10 ⁻²	2.6 x 10 ⁵	4.72 x 10 ⁻⁷	0.8	1.67 x 10 ⁶	2.23 x 10 ⁻⁶	1.92 x 10 ⁶	0.6
[110]	5.72 x 10 ¹	4.44 x 10 ³	3.94 x 10 ⁻⁶	0.9	7.87 x 10 ⁵	2.88 x 10 ⁻⁵	7.92 x 10 ⁵	0.7
[111]	3.46 x 10 ¹	1.21 x 10 ⁴	1.88 x 10 ⁻⁶	0.8	2.45 x 10 ⁴	6.33 x 10 ⁻⁴	3.77 x 10 ⁴	0.6

In these tables, R_p, the polarization resistance, is the sum of R_s, R_{ct} and R_f. It is clear from these tables that the resistance of the corrosion products film, R_f, is higher than that for the charge transfer, R_{ct}, which indicates that the corrosion resistance of these materials is due to the formed passive layer on top of their surface. Also, the R_p value for the polycrystalline material is lower than that obtained for monocrystals for up to three orders of magnitude, which indicates that the corrosion resistance of single crystals is higher than that for the polycrystal. Finally, an n_f value close to 1 indicates a low surface roughness due to a low corrosion rate value. On the other side, an n_f value close to 0.5 indicates high roughness of the surface due to a high dissolution rate. The n_f values for polycrystal in tables 3 and 4 are close to 0.5, which indicates a high corrosion rate, whereas that for single crystals were higher than 0.5, even close to 1, indicating a low corrosion rate.

3.4 EN measurements.

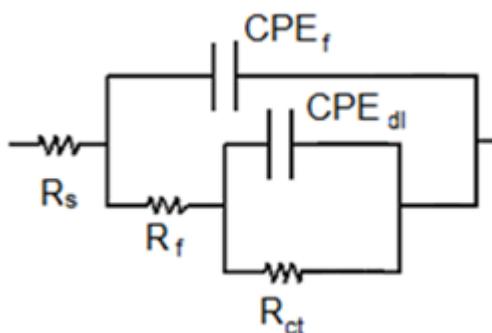


Figure 5. Equivalent circuits used to fit the EIS experimental data for Mo₃Si polycrystal and single crystals immersed in 0.05 M NaCl.

The time serie for the electrochemical noise in current (ENC) and in potential (ENP) for the polycrystal and the [100] single crystal are shown in Figs. 5 and 6. In 0.05 M NaCl solution, Fig. 5, time serie for the polycrystalline material, Fig. 5 a) and b) consist of transients with high intensity and high frequency, typical of a material undergoing localized type of corrosion such as pitting. An increase in the current transients in the anodic direction represents the breakdown of the protective film whereas

a decay in its value represents the rehealing of the protective film [24]. A similar behaviour was observed by the transients of the [100] monocrystal, Fig. 5 c) and d), however their intensity and frequency were much lower than those exhibited by polycrystal. A behaviour similar to he described was oserved in 0.5 M NaCl solution, Fig. 6, although in this case, the transients observed by [100] monocrystal were of lower intensity and high frequency, typical of a material either passivated or undergoing a uniform type of corrosion.

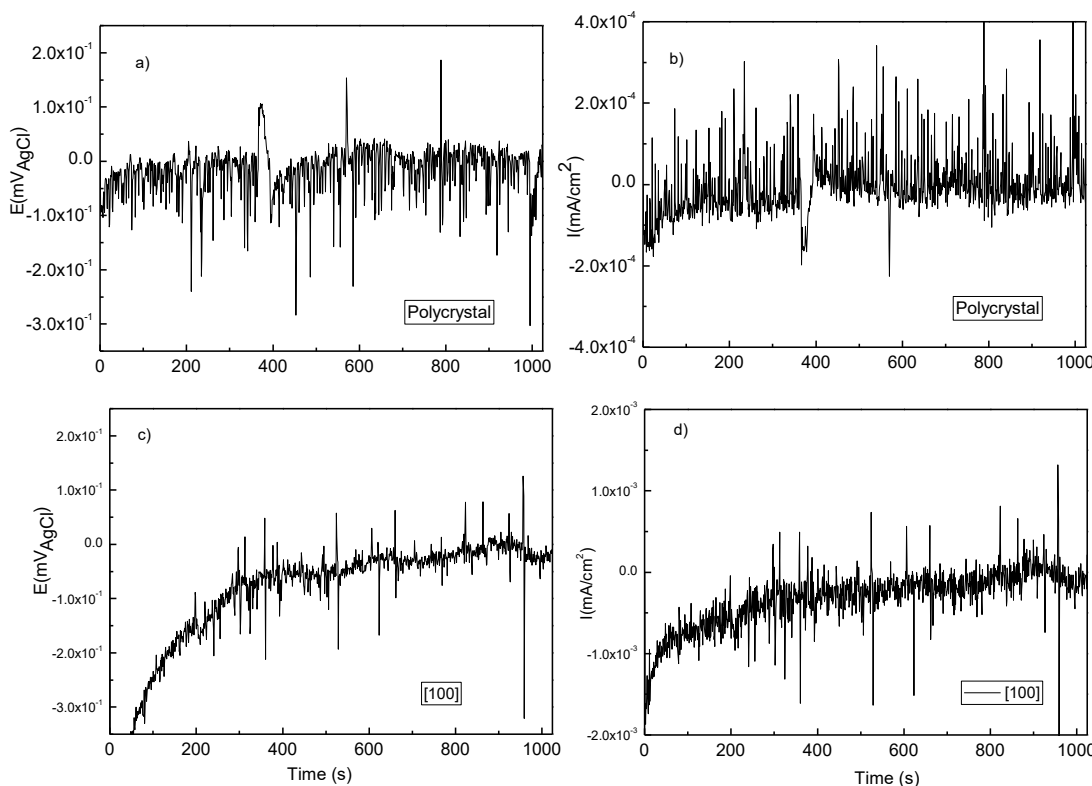


Figure 6. Time series for the noise in current and in potential for Mo₃Si polycrystal (a and b) and [100] single crystal (c and d) immersed in 0.05 M NaCl.

Polarization curve for [100] monocrystal in this solution, Fig. 2, indicated an active behaviour, without evidence of a passive layer, and this behaviour is observed in the ENC and ENP data shown in Fig. 7 c) and d). From the combined use of these data, a parameter called “noise resistance, R_n” was calculated through the estimation of the ratio of the standard deviation in potential, σ_v, and the standard deviation in current, σ_i, based on equation 3.1 [25, 26].

$$R_n = \frac{\sigma_v}{\sigma_i} \tag{2}$$

Similarly, the Localization index, LI, which denotes the susceptibility of a metal to localized corrosion, can be calculated by dividing the standard deviation in current, σ_i, by the root mean square value of the current (RMS_I) according to equation [27] :

$$LI = \sigma_i / RMS_I \tag{3}$$

A value of LI between 0.1 and 1 indicates a great susceptibility of metal to a localized type of corrosion. A value of LI between 0.1 and 0.01 indicates that the metal is susceptible to a mixed type of

corrosion. Finally, a value of LI between 0.01 and 0.001 indicates that the metal is susceptible to a uniform type of corrosion [27].

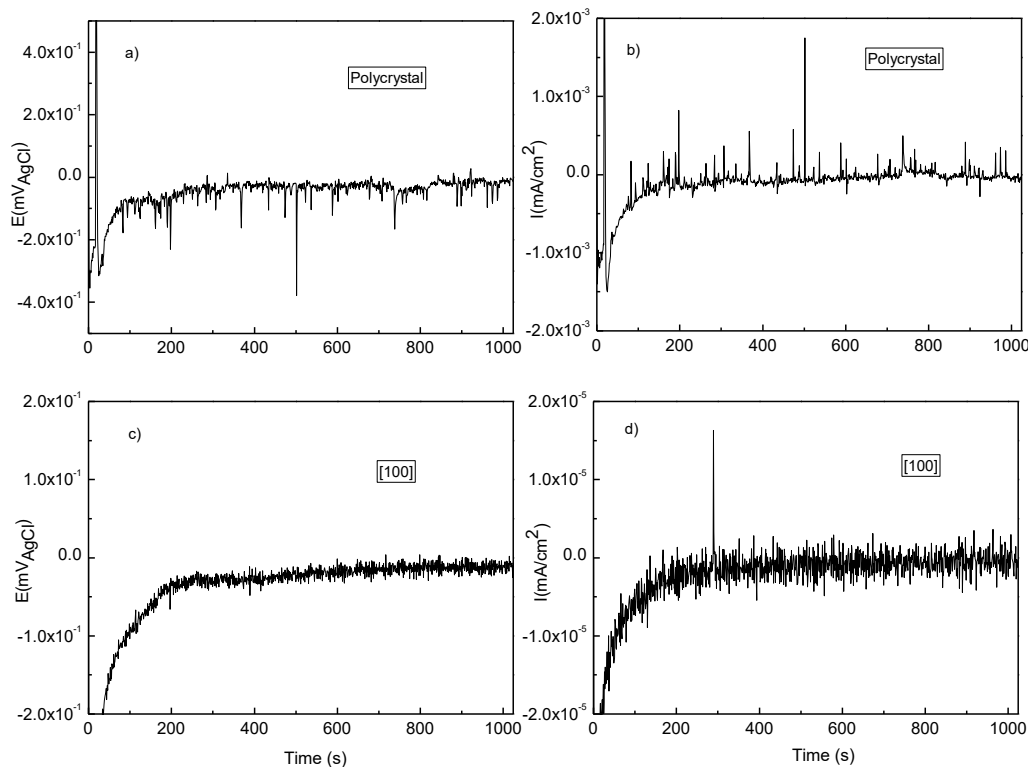


Figure 7. Time series for the noise in current and in potential for Mo₃Si polycrystal (a and b) and [100] single crystal (c and d) immersed in 0.5 M NaCl.

Table 5. Obtained values from electrochemical noise analysis for Mo₃Si polycrystal and single crystals immersed in 0.05 M NaCl.

Sample	R _n (Ωcm ²)	LI	σ _i (mA/cm ²)	σ _v (mV)
Polycrystal	3.04 x 10 ²	0.8	2.64 x 10 ⁻⁴	8.04 x 10 ⁻²
[100]	9.00 x 10 ²	0.9	4.03 x 10 ⁻⁵	3.63 x 10 ⁻²
[110]	4.38 x 10 ²	0.6	4.42 x 10 ⁻⁵	1.93 x 10 ⁻²
[111]	6.12 x 10 ²	0.5	2.84 x 10 ⁻⁵	1.74 x 10 ⁻²

Table 6. Obtained values from electrochemical noise analysis for Mo₃Si polycrystal and single crystals immersed in 0.5 M NaCl.

Sample	R _n (Ω cm ²)	LI	σ _i (mA/cm ²)	σ _v (mV)
Polycrystal	2.31 x 10 ²	0.8	2.81 x 10 ⁻⁴	6.50 x 10 ⁻²
[100]	1.29 x 10 ⁴	0.7	3.90 x 10 ⁻⁶	5.03 x 10 ⁻²
[110]	6.21 x 10 ²	0.8	1.59 x 10 ⁻⁵	9.86 x 10 ⁻³
[111]	5.51 x 10 ²	0.9	3.24 x 10 ⁻⁴	1.78 x 10 ⁻²

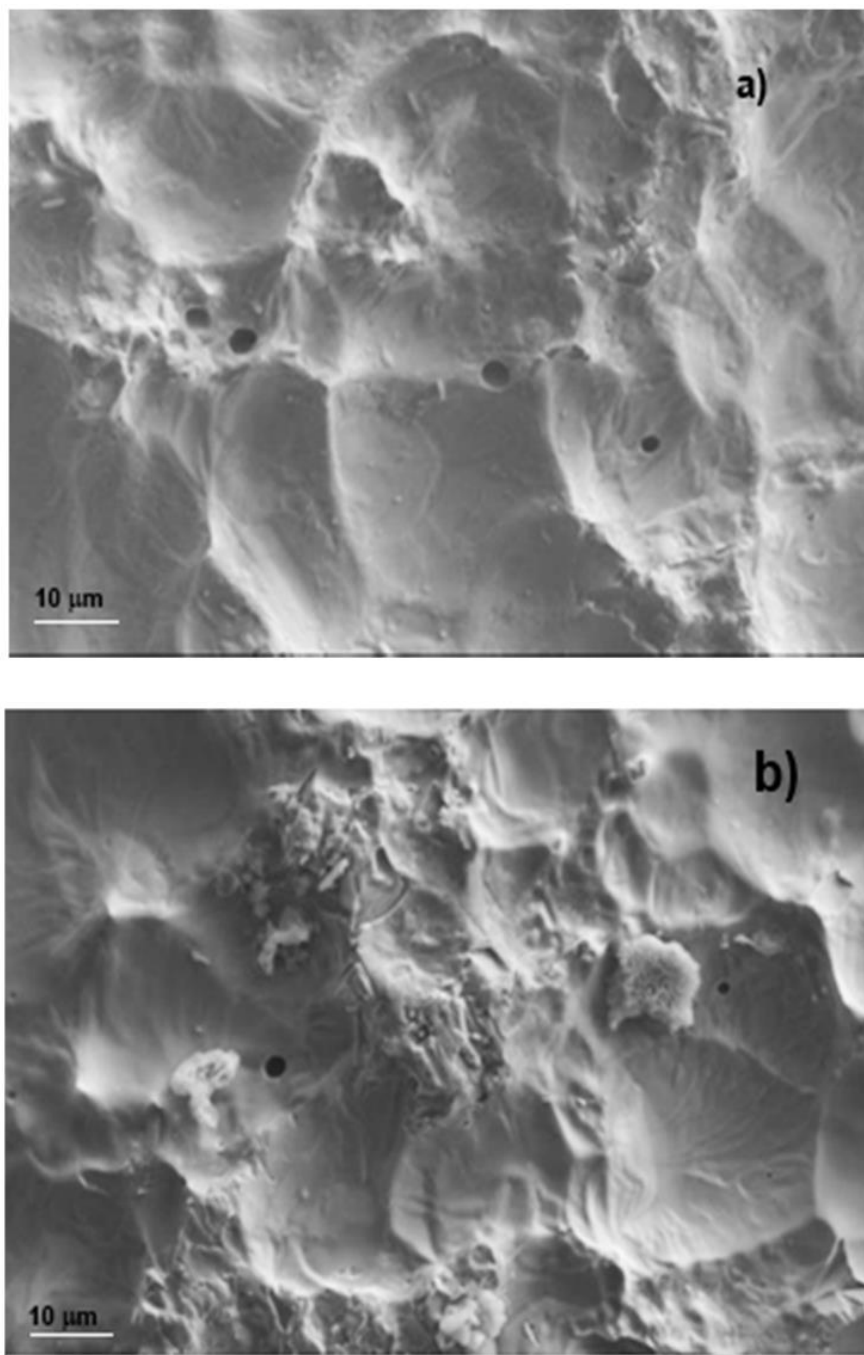


Figure 8. SEM micrograph of the Mo₃Si polycrystal after electrochemical measurements immersed in 0.05 and 0.5 M NaCl solution.

Tables 5 and 6 show the results from this analysis. The noise resistance value, R_n , equivalent to the polarization resistance value, R_p , were higher for single crystals in both solutions, which corroborate the obtained results from polarization curves and EIS measurements, which indicated their higher corrosion resistance than that for polycrystal. The values for σ_v and σ_i were higher for polycrystal also in both solutions, indicating that, in average, the noise transients in both potential and in current were higher for this material, and therefore, a higher corrosion rate. The LI values indicate

that all these materials are highly susceptibility to pitting type of corrosion. This was corroborated in Fig.8 where some micrographs of polycrystalline material corroded in both solutions clearly show localized type of corrosion such as pitting.

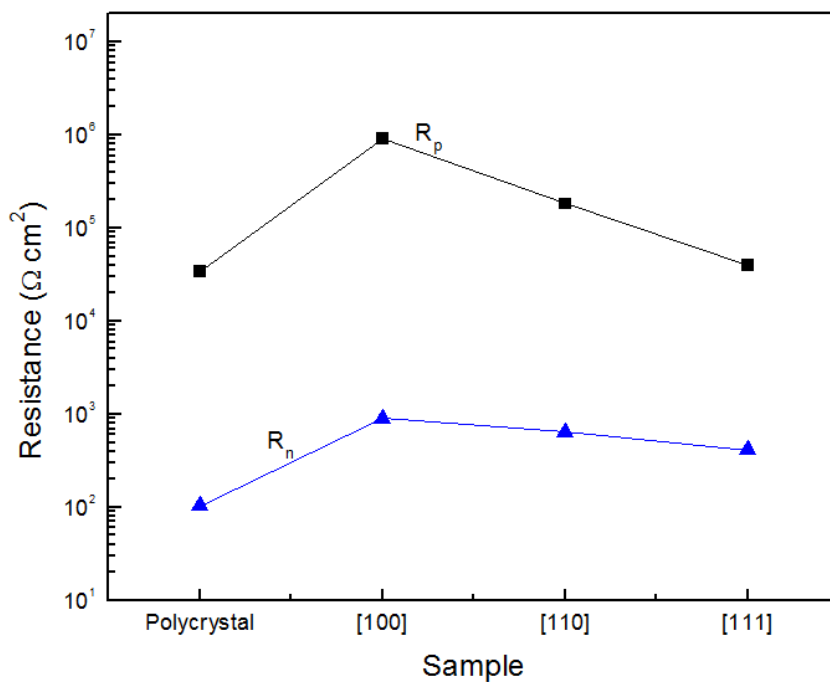


Figure 9. R_n , R_{sn} , and R_p values for Mo_3Si polycrystal and single crystals immersed in 0.05 M NaCl.

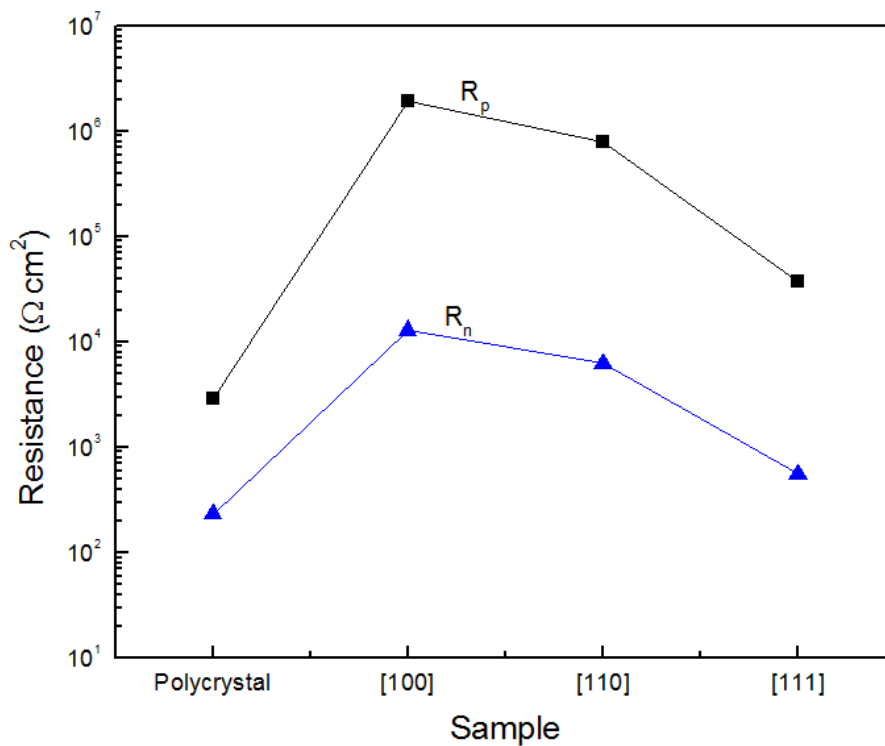


Figure 10. R_n , R_{sn} , and R_p values for Mo_3Si polycrystal and single crystals immersed in 0.5 M NaCl.

A summary of the results obtained by the different techniques in both solutions are given in Figs. 9 and 10, where the dependence of the different resistance values on the single crystals orientations and for the polycrystalline material is given. In both solutions, it can be seen the lowest R_p and R_n values, and thus, the highest corrosion rate, was obtained for the polycrystalline material, whereas the highest values were shown by the [100] single crystal, and decreased for the [110] and [111] ones. It is also clear that the R_n values were always lower than those for R_p , maybe because R_p is the sum of the solution resistance, R_s , the charge transfer resistance, R_{ct} , and the resistance of the corrosion products film, R_f , which are related to uniform type of corrosion, whereas R_n is only related with localized type of events such as break down of the protective film and its repassivation, pitting corrosion, etc...

4. CONCLUSIONS

The corrosion behavior of Mo_3Si single crystal in its crystal orientations, namely [100], [110] and [111] was evaluated in 0.05 and 0.5 M NaCl solutions. The same tests were performed with a polycrystalline material. Polarization curves indicated that polycrystalline material had the highest corrosion current density and the [100] single crystal exhibited the lowest value. EIS measurements indicated a corrosion resistance controlled by the corrosion resistance of the corrosion products film, indicating that the highest resistance film value, R_f , was for the [100] single crystal, whereas the lowest value was for the polycrystalline material. EN readings indicated that all the different silicides were susceptible to localized type of corrosion, being the polycrystalline material the most susceptible one.

References

1. X. Fan, T. Ishigaki and Y. Sato, *J. Mat. Res.*, 12 (2011) 1315.
2. K. Ito, H. Numakura, T. Hayashi, M. Yokobayashi and T. Murakami, *Met. Mat. Trans. A*, 36 (2005) 627.
3. R. Radhakrishnan, S. Bhaduri and C.H. Henager, *J. Min., Met. Mat. Soc.*, 49 (1997) 41.
4. L.I. Johansson, K.L. Hakansson, P.L. Wincott, U.O. Karlsson, and A.N. Christensen, *Phys. Rev. B: Cond. Mat.*, 43 (1991) 12355.
5. S. Krishnan, J. Dumbre, S. Bhatt, Esther T. Akinlabi, and R. Ramalingam, *Int. J. Mech., Aero., Ind., Manuf. Eng.*, 7 (2013) 649.
6. S. Wang and J. Wang, *Corros. Sci.*, 85 (2014) 183.
7. S. Ma, Z. Huang, J. Xing, G. Liu, Y. He, H. Fu, Y. Wang, Y. Li and D. Yi, *J. Mat. Res.*, 30 (2015) 257.
8. K.S. Shin, M.Z. Bian and N.D. Nam, *JOM*, 64 (2012) 664.
9. L. Fan, H. Lu, J. Leng, Z. Sun and C. Chen, *J. Power Sources*, 299 (2015) 66.
10. H. Fahamsyah Latief, Koji Kakehi and Xintao Fu, *Int. J. Electrochem. Sci.*, 7 (2012) 7608
11. J.E. Jackson, D.L. Olson, B. Mishra and A.N. Lasseigne-Jackson, *Int. J. Hydr. En.*, 32 (2007) 3789.
12. H. Chen, Q. Ma, X. Shao, J. Ma and B.X. Huang, *Corros. Sci.*, 70 (2013) 152.
13. P. Mandal, A.J. Thom, M.J. Kramer, V. Behrani and M. Akinc, *Mat. Sci. Eng.: A*, 371 (2004) 335.

14. I. Rosales, H. Martinez, D. Bahena, J.A. Ruiz, R. Guardian and J. Colin, *Corros. Sci.*, 51 (2009) 534.
15. J.G. Gonzalez-Rodriguez, I. Rosales, M. Casales, S. Serna and L. Martinez, *Mat. Sci. Eng. A*, 371 (2004) 217.
16. M. Herranen, A.D. Bauer, J.O. Carlsson and R.F. Bunshah, *Surf. Coat. Tech.*, 96 (1997) 245.
17. I. Rosales, *J. Cryst. Growth*, 310 (2008) 3833.
18. A.M. Shams and R.M. Saleh, *Metall. Angew Electrochem.*, 29 (1972) 184
19. G. Jangg, R. Kieffer and H. Kogler, *Werkst. Korr.*, 9(1970) 699
20. G. P. Halada, C. R. Clayton, H. Herman, S. Sampath and R. Tiwari, *J. Electrochem. Soc.*, 142 (1995) 74.
21. D. Horton, A. Zhu, J. Scully and M. Neurock, *MRS Comm.*, 4 (2014) 113.
22. T. Poornima, J. Nayak, and A. Nityananda Shetty, *Corros. Sci.*, 53 (2011) 3688.
23. H. Keles, M. Keles, I. Dehri and O. Serindag, *Mater. Chem. Phys.*, 112 (2008) 173.
24. J.C. Uruchurtu and J.L. Dawson, *Corrosion*, 43 (1987) 19.
25. C. Gouveia-Caridade, M.I.S. Pereira and C.M.A. Brett, *Electrochim. Acta*, 49 (2004) 785.
26. J. Mojica, E. García, F.J. Rodríguez and J. Genescá, *Prog. Org. Coat.*, 42 (2001) 218.
27. A. Contreras, M. Salazar, A. Carmona and R. Galván-Martínez, *J. Mat. Res.*, 4 (2017) 1.

© 2018 The Authors. Published by ESG (www.electrochemsci.org). This article is an open access article distributed under the terms and conditions of the Creative Commons Attribution license (<http://creativecommons.org/licenses/by/4.0/>).